Monte-Carlo simulation of events with Drell-Yan lepton pairs from antiproton-proton collisions

A. Bianconi*
Dipartimento di Chimica e Fisica per l'Ingegneria e per i Materiali, Università di Brescia, I-25123 Brescia, Italy, and Istituto Nazionale di Fisica Nucleare, Sezione di Pavia, I-27100 Pavia, Italy

Marco Radici†
Dipartimento di Fisica Nucleare e Teorica, Università di Pavia, and Istituto Nazionale di Fisica Nucleare, Sezione di Pavia, I-27100 Pavia, Italy

The complete knowledge of the nucleon spin structure at leading twist requires also addressing the transverse spin distribution of quarks, or transversity, which is yet unexplored because of its chiral-odd nature. Transversity can be best extracted from single-spin asymmetries in fully polarized Drell-Yan processes with antiprotons, where valence contributions are involved anyway. Alternatively, in single-polarized Drell-Yan the transversity happens convoluted with another chiral-odd function, which is likely to be responsible for the well known (and yet unexplained) violation of the Lam-Tung sum rule in the corresponding unpolarized cross section. We present Monte-Carlo simulations for the unpolarized and single-polarized Drell-Yan $\bar{p}p^{(\uparrow)} \to \mu^+\mu^- X$ at different center-of-mass energies in both configurations where the antiproton beam hits a fixed proton target or it collides on another proton beam. The goal is to estimate the minimum number of events needed to extract the above chiral-odd distributions from future measurements at the HESR ring at GSI. It is important to study the feasibility of such experiments at HESR in order to demonstrate that interesting spin physics can be explored already using unpolarized antiprotons.

PACS numbers: 13.75.-n,13.85.-t,13.85.Qk,13.88.+e

I. INTRODUCTION

When studying the spin structure of hadrons, the best tool is represented by the spin asymmetry, defined by the ratio between the difference and the sum of differential cross sections obtained by flipping the spin of one of the involved polarized hadrons. For hadronic beams, spin asymmetries are known since a long time; historically, the first one was obtained at FERMILAB, where an anomalous large transverse polarization of the Λ produced in proton-nucleon annihilations was measured [1], surviving even at large values of the Λ transverse momentum. More recently, similar anomalously large asymmetries have been observed by the FNAL E704 [2] and STAR [3] collaborations in inclusive pion production from collisions of transversely polarized protons. Such asymmetries require a nonvanishing imaginary part in the off-diagonal block of the fragmentation matrix of quarks into the detected hadron, which is forbidden in perturbative QCD at leading twist [4]. Soon after the first FERMILAB observation, a pioneering work appeared [5] about the possibility of having leading-twist asymmetries in fully polarized Drell-Yan processes, based on a new partonic function describing the quark transverse spin distribution in a transversely polarized hadron: the transversity. However, this work was basically ignored (and the observed asymmetries left unexplained) upon the prejudice that transverse-spin effects have to be suppressed. Only almost a decade later, it was realized that the transversity is connected to a helicity flipping mechanism but it is still a leading-twist distribution, necessary to complete the knowledge of the nucleon spin structure [6, 7] (for a review, see also Refs. [8, 9]).

As such, the transversity is not diagonal in the parton helicity basis; since at leading twist helicity and chirality coincide, it is usually mentioned as a chiral-odd function. But in the transverse spin basis it is diagonal and can be given a probabilistic interpretation. To be precise, in a transversely polarized hadron it describes the probability difference for having a transversely polarized parton with spin parallel or antiparallel to the one of the parent hadron. The chiral-odd feature brings in negative and positive consequences. The transversity needs a chiral-odd partner in order to be measured in a (chiral-even) cross section. At leading twist, the partner can be the transversity itself (for the corresponding antiquark in the aforementioned polarized Drell-Yan) or another chiral-odd unknown

*Electronic address: andrea.bianconi@bs.infn.it
†Electronic address: radici@pv.infn.it

fragmentation function in a semi-inclusive process. In particular, the transversity is not accessible in inclusive Deep-Inelastic Scattering (DIS) [10]. Therefore, in the Quark Parton Model (QPM) description of DIS, it does not have a counterpart at the level of structure function. Even if it depends on spin, it is not related to some partonic fraction of the hadron spin; the related twist-2 tensor operator $\sigma^{\mu\nu}\gamma_5$ is not part of the hadron full angular momentum tensor, and its first moment, the tensor charge, has a nonvanishing anomalous magnetic moment: contrary to the nonsinglet axial charge, from a starting input scale the tensor charge unavoidably evolves to zero [8].

If the hadron target has spin $\frac{1}{2}$, there is no transversity for gluons because of the mismatch in the change of helicity units. Hence, during evolution the quark transversity decouples from any radiative gluon. Moreover, it changes sign under charge conjugation, which implies that again during evolution it does not receive any contribution from charge-even structures like the $q\bar{q}$ pairs from the Dirac sea. In summary, the very same features that make the transversity quite an elusive object, are responsible for its very peculiar behaviour. Its evolution is similar to the one of a nonsinglet structure function; it describes the spin distribution of a valence quark while "switching off the contribution of gluons and of the vacuum" [8].

The growing interest in the transversity reflected in a rich experimental program, that led to some first recent measurements with hadronic [11] and leptonic beams [12, 13, 14, 15]. However, the field is confronted with rapid developments that should bring new upgraded and precise results in the near future [16]. Transverse spin is intimately connected with an explicit dependence of the parton distribution on its intrinsic transverse momentum. Including this explicit dependence, the list of parton distribution (and fragmentation) functions is very rich already at leading twist, containing also other chiral-odd objects [17]. While on the theoretical side the discussion is focussed on extending the universality proof to such functions [18, 19, 20, 21, 22], new azimuthal asymmetries are being deviced and measured both on the phenomenological [23, 24, 25] and experimental [26] side, that can shed light on new underlying mechanisms, ultimately related to the orbital motion of the quarks in the parent hadron.

In principle, the aforementioned polarized Drell-Yan is the most convenient process to measure the transversity at leading twist, because it does not involve other unknown functions. However, a Next-to-Leading (NLO) simulation has shown that the QCD evolution and the Soffer inequality (if forced to be fulfilled at any scale during evolution) make the resulting spin asymmetry very small [27, 28]. Moreover, the latter involves the transverse spin distribution of an antiquark in a transversely polarized proton, which is not expected to be large. This difficulty can be overcome at the foreseen HESR ring at GSI, where (polarized) antiprotons will be produced [29, 30, 31, 32, 33]: in the process $\bar{p}^{\uparrow}p^{\uparrow} \to l^+l^-X$, only valence (anti)quark distributions are involved without any further suppression.

But interesting information on the partonic spin structure of hadrons can also be inferred by using unpolarized antiproton beams only. In fact, in single-polarized Drell-Yan like $\bar{p}p^{\uparrow} \to l^+l^-X$ the polarized part of the cross section contains at leading twist three terms of which two produce interesting azimuthal spin asymmetries [34]. The first one involves the convolution of the standard unpolarized distribution f_1 with the Sivers function $f_{1T}^{\perp}$ [35], which describes how the distribution of unpolarized quarks is affected by the transverse polarization of the parent proton. The very same $f_{1T}^{\perp}$ appears at leading twist in semi-inclusive DIS processes like $lp^{\uparrow} \to l'\pi X$ [36] or $pp^{\uparrow} \to \pi X$ [37], and it is responsible of an azimuthal asymmetric distribution of the detected pions depending on the direction of the target polarization, the socalled Sivers effect. A measurement of a nonvanishing asymmetry would be a direct evidence of the orbital angular momentum of quarks [16].

The second term in the single-polarized Drell-Yan cross section has a different azimuthal dependence and it involves the transversity h_1 convoluted with the chiral-odd distribution $h_1^{\perp}$ [34], which describes the influence of the quark transverse polarization on its momentum distribution inside an unpolarized parent hadron. Extraction of the latter is of great importance, because $h_1^{\perp}$ is believed to be responsible for the well known violation of the Lam-Tung sum rule [38, 39, 40], an anomalous big azimuthal asymmetry of the corresponding unpolarized Drell-Yan cross section, that neither NLO QCD calculations [41], nor higher twists or factorization-breaking terms in NLO QCD [42, 43, 44] are able to justify.

In this paper, we will present numerical simulations for the unpolarized and single-polarized Drell-Yan process $\bar{p}p^{(\uparrow)} \to \mu^+\mu^-X$ at several center-of-mass energies using both configurations where the antiproton beam hits a fixed proton target or it collides on another proton beam. The goal is to estimate the minimum number of events needed to make the extraction of h_1 and $h_1^{\perp}$ feasible in future measurements at the HESR ring at GSI. In Sec. II, the kinematics and the general cross section formulae are reviewed. In Sec. III, details about the numerical simulation are given and results are presented in Sec. IV. Finally, some remarks and conclusions are drawn in Sec. V.

II. THE GENERAL FRAMEWORK

In a Drell-Yan process, two (polarized) hadrons H_1 and H_2, carrying momentum P_1 and P_2 with $P_{1(2)}^2 = M_{1(2)}^2$ (and spin S_1, S_2, such that $S_{1(2)}^2 = -1,\ P_{1(2)} \cdot S_{1(2)} = 0$), annihilate into a lepton l and an antilepton $\bar{l}$ with momenta

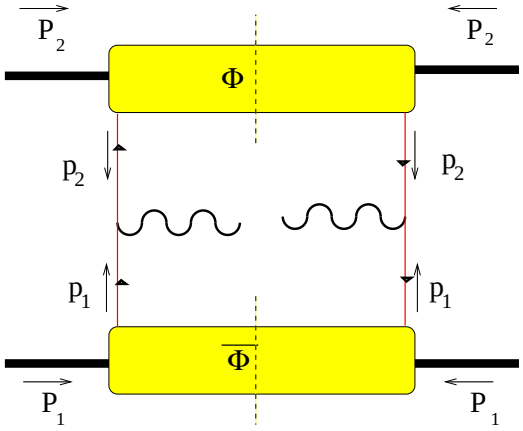

FIG. 1: The leading-twist contribution to the Drell-Yan process.

k_1 and k_2 (with $k^2_{1(2)} \sim 0$). The available initial squared energy in the center-of-mass (cm) frame is $s = (P_1 + P_2)^2$. The time-like momentum transfer defines the hard scale and it is directly related to the invariant mass of the final state, i.e. $q^2 \equiv Q^2 = (k_1 + k_2)^2 \geq 0$. Therefore, it is also indicated as $Q^2 \equiv M^2$; we will use both notations, in the following. The DIS regime is defined by the limit $Q^2, s \to \infty$, but keeping the ratio $0 \leq \tau = Q^2/s \leq 1$ limited. In this regime, the Drell-Yan process can be factorized into an elementary annihilation process, convoluted with two soft functions describing the distribution of the two annihilating partons inside the corresponding hadrons.

If M is constrained inside a range where the elementary annihilation can be safely assumed to proceed through a virtual photon converting into the final $l\,\bar{l}$ pair, while exploring the largest available range for τ, the dominant contribution at leading order is depicted in Fig. 1 [5], where the blobs represent the correlation functions for the annihilating antiparton (labelled "1") and parton (labelled "2"), respectively:

$$\begin{aligned} \bar{\Phi}(p_1; P_1, S_1) &= \int \frac{d^4z}{(2\pi)^4}\, e^{-ip_1\cdot z}\, \langle P_1 S_1|\psi(z)\,\bar{\psi}(0)|P_1, S_1\rangle\ , \\ \Phi(p_2; P_2, S_2) &= \int \frac{d^4z}{(2\pi)^4}\, e^{ip_2\cdot z}\, \langle P_2, S_2|\bar{\psi}(0)\,\psi(z)|P_2, S_2\rangle\ . \end{aligned} \tag{1}$$

When $Q^2 \to \infty$, the hard scale selects a light-cone dominant component for the hadron momenta, namely P_1^+ and P_2^-. Then, the parton momenta $p_{1(2)}$ are approximately aligned with the corresponding $P_{1(2)}$ and are given by the light-cone fractions

$$x_1 = \frac{p_1^+}{P_1^+} \simeq \frac{Q^2}{2\,P_1\cdot q}\ ,\ x_2 = \frac{p_2^-}{P_2^-} \simeq \frac{Q^2}{2\,P_2\cdot q}\ ,\ 0 \leq x_{1(2)} \leq 1\ , \tag{2}$$

while $q^+ = p_1^+$ and $q^- = p_2^-$, by momentum conservation [34].

As already anticipated in Sec. I, it is crucial to keep memory of the intrinsic transverse-momentum dependence inside the correlations functions of Eq. (1). Hence, the cross section will be kept differential in $\mathbf{q}_T$, which is bounded to $\mathbf{q}_T = \mathbf{p}_{1T} + \mathbf{p}_{2T}$ by momentum conservation; $\mathbf{p}_{iT}$ is the transverse component of the parton momentum p_i with respect to the axis defined by the corresponding hadron 3-momentum $\mathbf{P}_i$, with $i = 1, 2$. In this context, if $\mathbf{q}_T \neq 0$ the annihilation direction is not known. Hence, it is convenient to select the socalled Collins-Soper frame [45] (see fig. 2), where

$$\begin{aligned} \hat{t} &= \frac{q}{Q} \\ \hat{z} &= \frac{x_1 P_1}{Q} - \frac{x_2 P_2}{Q} \\ \hat{h} &= \frac{q_T}{|\mathbf{q}_T|}\ . \end{aligned} \tag{3}$$

The azimuthal angles lie in the plane perpendicular to $\hat{t}$ and $\hat{z}$. In particular, ϕ, ϕ_{S_i}, are the angles of $\hat{\mathbf{h}}, \mathbf{S}_{iT}$, $(i = 1, 2)$ with respect to the lepton plane, respectively, and $k^\mu_{i\perp} = (g^{\mu\nu} - \hat{t}^\mu\hat{t}^\nu + \hat{z}^\mu\hat{z}^\nu)k_{i\nu}$ the perpendicular component of k^μ_i, with $i = 1, 2$. Moreover, the cross section will be kept differential also in the solid angle for the lepton production,

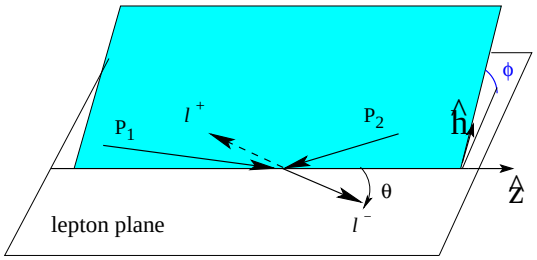

FIG. 2: The Collins-Soper frame.

i.e. $d\Omega = 2dyd\phi$, where the invariant $y = k_1^-/q^-$ reduces to $(1+\cos\theta)/2$ in the Collins-Soper frame, with θ defined in Fig. 2.

The hadronic tensor is obtained by taking the trace of the above correlation functions, after integrating upon the corresponding suppressed light-cone directions:

$$W^{\mu\nu} = \frac{1}{3}\int dp_1^- dp_2^+ \,\mathrm{Tr}\left[\bar\Phi(p_1;P_1,S_1)\,\gamma^\mu\,\Phi(p_2;P_2,S_2)\,\gamma^\nu\right]\Big|_{p_1^+=x_1P_1^+,\,p_2^-=x_2P_2^-} + \left(\begin{array}{ccc} q & \leftrightarrow & -q \\ \mu & \leftrightarrow & \nu \end{array}\right) . \tag{4}$$

Using the leading-twist parametrization for $\bar\Phi$ and Φ with explicit dependence on $\mathbf{p}_{1_T}$ and $\mathbf{p}_{2_T}$ [46], respectively, the fully differential cross section for the unpolarized Drell-Yan process $H_1\,H_2 \to l\,\bar l\,X$ can be written as [34]

$$\begin{aligned}\frac{d\sigma^o}{d\Omega dx_1 dx_2 d\mathbf{q}_T} &= \frac{\alpha^2}{3Q^2}\sum_f e_f^2\left\{A(y)\,\mathcal{F}\left[\bar f_1^f\, f_1^f\right]\right. \\ &\left. +B(y)\,\cos 2\phi\,\mathcal{F}\left[\left(2\hat{\mathbf{h}}\cdot\mathbf{p}_{1_T}\,\hat{\mathbf{h}}\cdot\mathbf{p}_{2_T} - \mathbf{p}_{1_T}\cdot\mathbf{p}_{2_T}\right)\frac{\bar h_1^{\perp f}\,h_1^{\perp f}}{M_1\,M_2}\right]\right\},\end{aligned} \tag{5}$$

where α is the fine structure constant, e_f is the charge of a parton with flavor f, and

$$\begin{aligned}A(y) &= \left(\frac{1}{2} - y + y^2\right) \overset{\mathrm{cm}}{=} \frac{1}{4}\left(1+\cos^2\theta\right) , \\ B(y) &= y(1-y) \overset{\mathrm{cm}}{=} \frac{1}{4}\sin^2\theta\,.\end{aligned} \tag{6}$$

The functions f_1^f, $h_1^{\perp f}$, are the distributions of unpolarized and transversely polarized partons with flavor f in unpolarized hadrons, respectively. Both are convoluted with their antiparton partners according to the definition

$$\mathcal{F}\left[\bar f_1^f\, f_1^f\right] \equiv \int d\mathbf{p}_{1_T} d\mathbf{p}_{2_T}\,\delta\left(\mathbf{p}_{1_T}+\mathbf{p}_{2_T}-\mathbf{q}_T\right)\left[\bar f_1^f(x_1,\mathbf{p}_{1_T})\,f_1^f(x_2,\mathbf{p}_{2_T}) + (1\leftrightarrow 2)\right] . \tag{7}$$

The cross section (5) can be integrated upon the angular distribution and the transverse momentum of the final lepton pair,

$$\begin{aligned}\frac{d\sigma^o}{dx_1dx_2} &= \frac{1}{3}\sum_f e_f^2\,\frac{4\pi\alpha^2}{3Q^2}\left[\bar f_1^f(x_1)\,f_1^f(x_2) + (1\leftrightarrow 2)\right] \\ &= \frac{1}{3}\sum_f \int dQ^2\,\frac{d\hat\sigma^f}{dQ^2}\,\delta(\hat s - Q^2)\left[\bar f_1^f(x_1)\,f_1^f(x_2) + (1\leftrightarrow 2)\right] ,\end{aligned} \tag{8}$$

where, if neglecting the parton masses, $\hat s \sim x_1x_2s$ is the available cm energy for the elementary annihilation, and the elementary QPM cross section has been put into evidence. At this point, it is useful to recall that $\tau = x_1x_2$, and to introduce the new invariant $x_{_F} = x_1 - x_2$, which is the "longitudinal" momentum of the annihilating partons in their cm frame with respect to the maximum "longitudinal" momentum available. If $d\sigma^o$ is considered differential also in the leptonic invariant mass $Q^2 \equiv M^2$, by transforming from the set $\{x_1, x_2\}$ to the variables $\{\tau, x_{_F}\}$, and after integrating upon $d\tau$, we recover the well known result

$$M^4\,\frac{d\sigma^o}{dM^2dx_{_F}} = \frac{4\pi\alpha^2}{9}\,\frac{\tau}{x_1+x_2}\sum_f e_f^2\left[\bar f_1^f(x_1)\,f_1^f(x_2) + (1\leftrightarrow 2)\right] \tag{9}$$

about the scaling of the cross section in the cm energy s, which has been experimentally confirmed [47]. Interestingly, when considered differential in $\sqrt{\tau}$ and $x_{_F}$, the cross section falls like $\sim 1/s$; this remark will be reconsidered in the next Section because it influences the choice of the kinematical set-up.

When one of the annihilating hadrons is transversely polarized, i.e. for the single-polarized Drell-Yan $H_1\, H_2^\uparrow \to l\, \bar{l}\, X$, the polarized part of the cross section becomes [34]

$$\frac{d\Delta\sigma^\uparrow}{d\Omega dx_1 dx_2 d\mathbf{q}_{_T}} = \frac{\alpha^2}{3Q^2} \sum_f e_f^2\, |\mathbf{S}_{2_T}| \left\{ A(y)\, \sin(\phi - \phi_{S_2})\, \mathcal{F}\left[\hat{\mathbf{h}} \cdot \mathbf{p}_{2_T}\, \frac{\bar{f}_1^f\, f_{1T}^{\perp\, f}}{M_2} \right] \right.$$
$$- B(y)\, \sin(\phi + \phi_{S_2})\, \mathcal{F}\left[\hat{\mathbf{h}} \cdot \mathbf{p}_{1_T}\, \frac{\bar{h}_1^{\perp\, f}\, h_1^f}{M_1} \right]$$
$$\left. - B(y)\, \sin(3\phi - \phi_{S_2})\, \mathcal{F}\left[\left(4\hat{\mathbf{h}} \cdot \mathbf{p}_{1_T}\, (\hat{\mathbf{h}} \cdot \mathbf{p}_{2_T})^2 - 2\hat{\mathbf{h}} \cdot \mathbf{p}_{2_T}\, \mathbf{p}_{1_T} \cdot \mathbf{p}_{2_T} - \hat{\mathbf{h}} \cdot \mathbf{p}_{1_T}\, \mathbf{p}_{2_T}^2 \right) \frac{\bar{h}_1^{\perp\, f}\, h_{1T}^{\perp\, f}}{2M_1\, M_2^2} \right] \right\}, \qquad (10)$$

where $f_{1T}^{\perp\, f}$ is the Sivers function, describing the distribution of unpolarized partons with flavor f in a transversely polarized hadron, while $h_{1T}^{\perp\, f}$ describes the distribution of transversely polarized partons with flavor f in transversely polarized hadrons.

From Eq. (10), a spin asymmetry weighted by $\sin(\phi - \phi_{S_2})$ allows to isolate $f_{1T}^\perp$ through the known distribution f_1 with a mechanism similar to the Sivers effect in DIS with lepton beams [35]. Then, it could be possible to verify the interesting conjecture that the Sivers function should change sign when going from DIS to Drell-Yan [19], because of the different behaviour of the tower operator that must be inserted in Eq. (1) to link the space-time points 0 and z in order to make the whole correlator color-gauge invariant.

In Eq. (10), another interesting spin asymmetry is obtained by using the $\sin(\phi + \phi_{S_2})$ weight, because the transversity h_1 can be extracted with a mechanism similar to the Collins effect [48]. However, the convolution involves also the unknown chiral-odd function $h_1^\perp$, which luckily appears also in the leading-twist part of the unpolarized cross section (5). A combined analysis of the $\cos 2\phi$ and $\sin(\phi + \phi_{S_2})$ moments of azimuthal asymmetries for unpolarized and single-polarized Drell-Yan cross sections, respectively, should allow a complete determination of all the unknown distribution functions. The former asymmetry is particularly interesting because it could represent a natural explanation of the observed large azimuthal asymmetry of the cross section for the process $\pi^- A \to \mu^+ \mu^- X$, where A is either deuterium or tungsten, and the π^- beam energy ranges from 140, 194, 286 GeV [38, 39] to 252 GeV [40]. At leading order in α_s, the data can be parametrized as

$$\frac{1}{\sigma^o}\, \frac{d\sigma^o}{d\Omega} \equiv \left[\frac{\alpha^2}{3Q^2} \sum_f e_f^2 \int dx_1 dx_2 d\mathbf{q}_{_T}\, \mathcal{F}\left[\bar{f}_1^f\, f_1^f \right] \right]^{-1} \int dx_1 dx_2 d\mathbf{q}_{_T}\, \frac{d\sigma^o}{d\Omega dx_1 dx_2 d\mathbf{q}_{_T}}$$
$$= \frac{3}{4\pi}\, \frac{1}{\lambda + 3} \left(1 + \lambda\, \cos^2\theta + \mu\, \sin^2\theta \cos\phi + \frac{\nu}{2}\, \sin^2\theta \cos 2\phi \right), \qquad (11)$$

with $\lambda \sim 1$ and $\mu \ll \nu \sim 30$ % [38, 39]. Both Leading Order (LO) and Next-to-Leading Order (NLO) perturbative QCD calculations give $\lambda \sim 1$, but $\mu \sim \nu \sim 0$ [41]. Other mechanisms, like higher twists or factorization breaking terms at NLO, are not able to explain the size of ν in a consistent picture [42, 43, 44]. On the contrary, from Eq. (5) it is evident that a leading-twist (hence, large) azimuthal $\cos 2\phi$ asymmetry in the unpolarized cross section is possible thanks to the distribution $h_1^\perp$ [34]. Since the latter is defined to describe the transverse polarization of quarks in a unpolarized hadron, it is intimately connected to the orbital motion of the parton inside the hadron; the product $\bar{h}_1^\perp\, h_1^\perp$ should bring a change of two units in the orbital angular momentum, such that the angular dependence involves twice the azimuthal angle ϕ.

In the next Section, we will see how to numerically simulate these azimuthal asymmetries with a suitable Monte-Carlo.

III. MONTE-CARLO SIMULATIONS

In this Section we discuss a Monte-Carlo simulation for the specific processes $\bar{p}\, p \to \mu^+\, \mu^-\, X$ and $\bar{p}\, p^\uparrow \to \mu^+\, \mu^-\, X$. The primary goal of the simulation is to estimate the number of events required for such a Drell-Yan experiment in order to access unambiguous information on the distribution functions of interest, namely the transversity h_1 and $h_1^\perp$. Secondly, it is important also to clarify the role and the consequences of the unavoidable approximations and kinematical cuts.

The cross sections for the unpolarized and polarized processes, Eqs. (5) and (10), respectively, are valid only in the framework of the QPM. In order to implement QCD corrections (and to test the resulting formulae), we will heavily refer to conventions and results of Ref. [40], where a thorough analysis was performed on a large sample of muon pairs produced by a 252-GeV π^- beam interacting in a tungsten target. We will also use results from Ref. [49] and Ref. [34] in adapting the relations of Ref. [40] to the case of an antiproton beam (with some care in matching the different notations) and of a polarized target, respectively.

The Monte-Carlo events were generated from the following general expression for the cross section:

$$\frac{d\sigma}{d\Omega dx_{_F} d\tau d\mathbf{q}_{_T}} = K\,\frac{1}{s}\,A(\mathbf{q}_{_T}, x_{_F}, M)\,F(x_{_F}, \tau)\,\sum_{i=1}^{4} c_i(|\mathbf{q}_{_T}|, x_{_F}, \tau)\,S_i(\theta, \phi, \phi_{S_p})\;, \tag{12}$$

or, equivalently,

$$\frac{d\sigma}{d\Omega dx_{\bar{p}} dx_p d\mathbf{q}_{_T}} = K\,\frac{1}{s}\,A(\mathbf{q}_{_T}, x_{\bar{p}} - x_p, M)\,(x_{\bar{p}} + x_p)\,F'(x_{\bar{p}}, x_p)\,\sum_{i=1}^{4} c'_i(|\mathbf{q}_{_T}|, x_{\bar{p}}, x_p)\,S_i(\theta, \phi, \phi_{S_p})\;, \tag{13}$$

where the above mentioned scaling in $1/s$ has been put into evidence. As the reader can argue from the formulae of previous Section, a (QPM-inspired) factorized structure for the cross section, but still differential in $d\mathbf{q}_{_T}$, implies that some simplifying assumption has been made on the $\mathbf{p}_{_T}$ dependence of the distribution functions, such that the convolution (7) could be solved. The actual expression and its kinematical justification, as well as each other factor in the above equations, are separately discussed in the following.

A. Kinematics and the transverse-momentum dependence

For the handbag mechanism of Fig. 1 to be the dominant contribution, some kinematical contraints must be fulfilled. First of all, the cm energy s must be much bigger than the hadron masses involved. Secondly, in order to have a good control of the elementary annihilation process the invariant mass M of the muon pair must not overlap with the hadronic resonance spectrum. The most natural choice is to select M such that 4 GeV $\leq M \leq$ 9 GeV: in this range, between the ψ' and the first resonance of the Υ family, there should be no ambiguity in assuming that the elementary annihilation is followed by the creation of a virtual photon.

We will consider both options where the antiproton beam hits a fixed proton target or it collides on a proton beam. In the first case, if the target is at rest, we have

$$M^2 = \tau\, s = \tau\,(P_p + P_{\bar{p}})^2 = \tau\, 2M_p(M_p + E_{\bar{p}}) \sim \tau\, 2M_p E_{\bar{p}}\;; \tag{14}$$

near the limit $\tau \to 1$ (i.e., assuming that all the available cm energy flows into the final state), the upper limit for M would require a maximum antiproton beam energy of roughly 40 GeV. With the lower cutoff of $M > 4$ GeV, this corresponds to span the range $0.5 \lesssim \sqrt{\tau} \lesssim 1$, as discussed in the next Section and displayed in Fig. 3. Lower antiproton beam energies would reduce this scatter plot to an unrealistic small portion of phase space limited to very high values of both x_p and $x_{\bar{p}}$, unless releasing the constraint on the lower cutoff of the dilepton mass. In fact, for a beam energy of $E_{\bar{p}} = 15$ GeV it is also possible to cover a wide range of τ with the constraint 1.5 GeV $\leq M \leq$ 2.5 GeV, which grants no overlap with the positions of the ϕ and J/ψ resonances. Therefore, in the following we will use both energies for the antiproton beam.

Recently, the discussions about the optimal setup configuration for spin asymmetry measurements at the HESR at GSI have focussed also on the collider option where two beams of protons and antiprotons collide at much higher s, particularly in the socalled asymmetric mode with $E_p \neq E_{\bar{p}}$. Neglecting the hadron masses and in the same conditions as in Eq. (14), we have

$$M^2 \sim (P_p + P_{\bar{p}})^2 \sim 4E_p E_{\bar{p}}\;, \tag{15}$$

because now $\hat{\mathbf{P}}_p = -\hat{\mathbf{P}}_{\bar{p}}$. Hence, for the case of an antiproton beam energy of 15 GeV a proton beam of 3.3 GeV approximately gives $s \sim 200$ GeV^2. By keeping the above cutoffs for M, a large portion of the phase space for x_p and $x_{\bar{p}}$ can be explored, particularly at lower values. Moreover, at larger energies the elementary process should be less affected by higher-order corrections like subleading twists; hence, the theoretical description should be more clean. Finally, as discussed below in Sec. III D, the collider mode offers also the advantage that no dilution factors are introduced that affect the target polarization. For all these reasons, in the following we will present simulations for the single-polarized Drell-Yan process also at this kinematics.

The independent invariant fraction, $x_{_F} = x_{\bar{p}} - x_p$, can be redefined for practical purposes as [40]

$$x_{_F} \equiv \frac{2q_{_L}}{\sqrt{s}} \,, \tag{16}$$

where $q_{_L}$ indicates the longitudinal component of the virtual photon momentum (in the following, we will also use the notation $q_{_T} = |\mathbf{q}_{_T}|$). The definition (16) puts in explicit evidence the content of $x_{_F}$ being the fraction of the total available longitudinal momentum in the collision cm frame. In the DIS regime, it recovers the previous definition in terms of light-cone momentum fractions. It is important to note that the minimum and maximum $x_{_F}$ values depend on the energy. For the case of $E_{\bar{p}} = 40$ GeV and a fixed proton target, it turns out that $-0.7 \lesssim x_{_F} \lesssim 0.7$.

A factorized transverse-momentum dependence in the differential cross section is achievable assuming a simple parametrization for the $\mathbf{p}_{_T}$ dependence of the distribution functions (typically, Gaussian-like), which allows to directly calculate the convolution (7) and get a factorized product of two functions depending separately upon $\mathbf{q}_{_T}$ and $x_{_F}, \tau$ (or, equivalently, $x_{\bar{p}}, x_p$; see, for example, the discussion of Sec. V in Ref. [34]). Alternatively, since the input $\mathbf{p}_{_T}$ dependence and, consequently, the obtained $\mathbf{q}_{_T}$ dependence are purely phenomenological, a parametrization for the latter can be assumed *ab initio* to fit the data. For example, the following form has been used in Sec. V of Ref. [40], e.g.

$$A(q_{_T}, x_{_F}, M) = \frac{5\,\dfrac{a}{b}\,\left[\dfrac{q_{_T}}{b}\right]^{a-1}}{\left[1 + \left(\dfrac{q_{_T}}{b}\right)^{a}\right]^{6}} \,, \tag{17}$$

where $a(x_{_F}, M)$, $b(x_{_F}, M)$, are parametric polynomials given in App. A of the same reference. The normalization condition is

$$\int dq_{_T}\, A(q_{_T}, x_{_F}, M) = 1 \,. \tag{18}$$

The function (17) gives a good reproduction of the observed $q_{_T}$ spectrum for $\pi - p$ Drell-Yan events (see fig.23 of Ref. [40]). However, in Ref. [49] the same analysis has been repeated also for $\bar{p} - p$ events and the two distributions are similar for $q_{_T} \gtrsim 1$ GeV/c, while above 3 GeV/c big error bars prevent from any comparison. Therefore, we have adopted the same distribution (17) also in our analysis.

With the parametrization displayed in App. A of Ref. [40], a and b turn out to be smoothly dependent on $x_{_F}$ and M, while the calculated $\langle \mathbf{q}_{_T}^2 \rangle$ is a smooth function only in M (after integrating on the whole range of $x_{_F}$): it displays a strong decrease in $x_{_F}$ for $x_{_F} \to 0.7$ after averaging on the whole range of M. The smooth dependence of $\langle \mathbf{q}_{_T}^2 \rangle$ on M reflects in its experimentally observed scale dependence $\sim \sqrt{s}$, but if the cut-offs in the invariant mass are the same for two experiments at different energies (as it is the case between the measurement of Ref. [40] and the present simulation), the average squared transverse momentum results approximately the same.

We have cut the $q_{_T}$ distribution from below, because events at low $q_{_T}$ do not contribute to the spin asymmetry, but rather to the background, and they would represent a sort of artificial dilution factor. However, since this cutoff has drastic consequences on the final number of available events, a good compromise at these energies is represented by $q_{_T} > 1$ GeV/c, in accordance with several previous experimental observations. Such a constraint implies a reduction of the total number of available events by approximately 50%.

B. QCD corrections and the partonic-momentum dependence

The well established experimental observation that Drell-Yan pairs are distributed with $\langle q_{_T} \rangle > 1$ GeV/c and depending on $\sqrt{s}$, suggests that sizeable QCD corrections are needed on top of the QPM, because confinement alone induces much smaller quark intrinsic transverse momenta. The Feynman diagrams typically involve $q\bar{q}$ annihilations into gluons or quark-gluon scattering (see Fig. 3 of Ref. [40]). They have been calculated introducing two main levels of approximation [50, 51]. The first one is the so-called Leading-Log Approximation (LLA), where the leading logarithmic corrections to the Drell-Yan cross section can be resummed at any order in the strong coupling constant α_s, with the final net effect that the parton distribution functions get an additional scale dependence on M^2. Following the prescriptions of Ref. [52], the DGLAP evolution could be obtained by describing the functions with parameters explicitly depending on $\log M^2$ (see Apps. A,B and D in Ref. [40] for further details). However, since the M range explored in Ref. [40] is practically the same assumed here, also the same parametrization described there in App. A is here retained; correspondingly, the function F' in Eq. (13) does no longer depend on the scale M^2. We have explicitly verified that starting from the parametrization of Ref. [40] (and after a suitable transformation due to

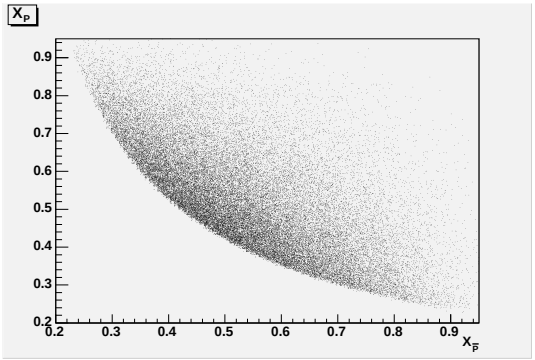

FIG. 3: The scatter plot for 48000 events of Drell-Yan muon pairs produced by the collision of a 40 GeV antiproton beam on a proton target in the kinematic conditions discussed in the text.

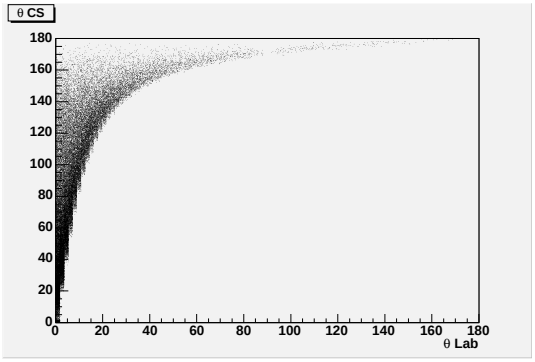

FIG. 4: The correlation between the polar angle of μ^+ in the laboratory, $\theta_{\rm lab}$, and in the Collins-Soper frame, θ, for the collision of antiprotons with 40 GeV energy and fixed proton targets.

different conventions), our Monte-Carlo gives a good approximation of the results of Ref. [49] with an antiproton beam of 125 GeV.

The function F' in Eq. (13) is given by

$$F'(x_{\bar p}, x_p) = \frac{\alpha^2}{3Q^2} \sum_f e_f^2 \, \bar f_1^f(x_{\bar p}) \, f_1^f(x_p) + (\bar p \leftrightarrow p) \, , \tag{19}$$

namely it is the symmetric part of the unpolarized cross section that has been factorized out for convenience (see Eq. (5)). With $f_1(x)$ parametrized as in App. A of Ref. [40] for the various flavors $f = u, d, s$, we show in Fig. 3 the scatter plot in $x_{\bar p}$ and x_p of some 48000 events sorted by the cross section of Eq. (13) including Eq. (19) and assuming the kinematics corresponding to $E_{\bar p} = 40$ GeV with the cutoffs $q_{_T} > 1$ GeV/c, $4 \le M \le 9$ GeV and $-0.7 \lesssim x_{_F} \lesssim 0.7$.

The line bisecting the plot at 45 deg. corresponds to $x_{_F} = 0$; parallel lines above and below it indicate $x_{_F} > 0$ and $x_{_F} < 0$, respectively. Hyperboles with $x_{\bar p} x_p = $ const. select various values of τ: moving to the upper right corner of the figure corresponds to the limit $\tau \to 1$, where events are rare; on the contrary, approaching the lower cutoff $\sqrt{\tau} \sim 0.5$ the distribution becomes much more dense. Nevertheless, the projection along each axis displays a significant number of events also at the boundary values of $x_{\bar p}, x_p$. They correspond to large positive and negative values of $x_{_F}$, which in turn indicate, in the Collins-Soper frame, small and large values of the muon pair polar angle θ, respectively. For a fixed target and in the laboratory frame, since we have antipartons in the beam and partons in the target, large and positive values of $x_{_F}$ correspond to "forward" events where, by convention, the polar angle $\theta_{\rm lab}$ of μ^+ is small. Viceversa, large negative values of $x_{_F}$ correspond to "backward" events with large $\theta_{\rm lab}$. This is at variance with the experiments of Refs. [40, 49], where events with only large positive $x_{_F}$ were collected because of the higher beam energy and of the stronger absorption of the unpolarized target. In Fig. 4, the correlation between θ and $\theta_{\rm lab}$ is shown in order to estimate the possible geometry of the apparatus for detecting the muons. The points are spread because the relation between the two frames depends on $x_{\bar p}, x_p$, and $q_{_T}$.

The second level of approximation in the QCD corrections to the QPM result is referred to as Next-to-Leading-Log Approximation (NLLA). It amounts to include in the calculation all processes at first order in α_s involving a quark,

an antiquark and a gluon [50, 51]. The effect is large, because the cross section has approximately twice the size of the corresponding one in the QPM. This correction turns out to be roughly independent of $x_{_F}$ and M^2 (except for the kinematical upper limits) and it is usually indicated as the K factor. As explained in Ref. [49], K depends on the choice of the parametrization of the distribution functions through their normalization, but it also grows like $\sqrt{\tau}$ [40]. However, in the following we will consider azimuthal asymmetries, which are defined as ratios of cross sections. Hence, it is legitimate to expect that such corrections in the numerator and in the denominator approximately compensate each other. Indeed, for fully polarized Drell-Yan reactions at high energy the spin asymmetry is weakly affected by QCD corrections [27]. In any case, for the considered antiproton energy $E_{\bar{p}} = 40$ GeV at $\sqrt{\tau} \sim 0.5$, where most of the events are concentrated, the best compromise is to assume the constant value $K = 2.5$.

C. The angular distribution

If the orientation of the $\hat{x}$ axis of the Collins-Soper frame (pointing along $\mathbf{q}_{_T}$) with respect to the laboratory frame is indicated with ϕ^l, then it turns out that $\phi^l = -\phi_{S_p}$ because, in practice, the latter angle gives the position of the $\hat{x}$ axis of the laboratory frame (pointing along $\mathbf{S}_{p_T}$) in the Collins-Soper frame. The whole solid angle (θ, ϕ) of the final muon pair in the Collins-Soper frame is randomly distributed in each variable. The explicit form for sorting the angular distribution in the Monte-Carlo is

$$\begin{aligned}\sum_{i=1}^{4} c_i'(q_{_T}, x_{\bar{p}}, x_p)\, S_i(\theta, \phi, \phi_{S_p}) \;&=\; 1 + \cos^2\theta \\ &\quad + \frac{\nu(x_{\bar{p}}, x_p, q_{_T})}{2}\, \sin^2\theta\, \cos 2\phi \\ &\quad + |\mathbf{S}_{p_T}|\, c_4(q_{_T}, x_{\bar{p}}, x_p)\, S_4(\theta, \phi, \phi_{S_p})\;, \end{aligned} \tag{20}$$

which corresponds to the parametrization (11) for $\lambda = 1, \mu = 0$, as suggested by experimental observations, and includes also a polarized term as suggested by Eq. (10).

If quarks were massless, the virtual photon would be only transversely polarized and the angular dependence would be described by the functions $c_1 = S_1 = 1$ and $c_2 = 1$, $S_2 = \cos^2\theta$. Violations of such azimuthal symmetry induced by the function $c_3 \equiv \frac{\nu}{2}$ are due to the longitudinal polarization of the virtual photon and to the fact that quarks have an intrinsic transverse momentum distribution. QCD corrections influence such function, which in principle depends also on $x_{\bar{p}}, x_p$, and M^2 (see App. A of Ref. [40]). In practice, we follow Ref. [34] (where $\nu = 2\kappa$ and κ is given in Sec. V) and assume the simple form

$$\nu(q_{_T}) = 3.5\, \frac{4M_{_C}^2 q_{_T}^2}{(4M_{_C}^2 + q_{_T}^2)^2}\;, \tag{21}$$

where $M_{_C} = 2.3$ GeV.

The last term in Eq. (20) corresponds to the polarized part of the cross section, which is fully described in Eq. (10). Since we are interested in the convolution of h_1 and $h_1^\perp$, we assume that the angular dependence of the azimuthal spin asymmetry is given by

$$S_4(\theta, \phi, \phi_{S_p}) = \sin^2\theta\, \sin(\phi + \phi_{S_p})\;. \tag{22}$$

Recalling that in Eq. (13) the azimuthally symmetric unpolarized part $F'(x_{\bar{p}}, x_p)$ of the cross section has been factorized out, the corresponding coefficient c_4 in Eq. (20) becomes

$$c_4(q_{_T}, x_{\bar{p}}, x_p) = -\frac{\sum_f e_f^2\, \mathcal{F}\left[\hat{\mathbf{h}}\cdot\mathbf{p}_{\bar{p}_T}\, \frac{\bar{h}_1^{\perp f}\, h_1^f}{M_{\bar{p}}}\right]}{\sum_f e_f^2\, \mathcal{F}\left[\bar{f}_1^f\, f_1^f\right]}\;. \tag{23}$$

Following Ref. [34], we introduce some model assumptions on the behaviour of the unknown $h_1^\perp(x, \mathbf{p}_{_T})$. Its $\mathbf{p}_{_T}$ dependence is of the Gaussian type, while the x dependence is given directly by $f_1(x)$:

$$h_1^{\perp f}(x, \mathbf{p}_{_T}^2) = \frac{\alpha_{_T}}{\pi}\, \frac{M_{_C}}{\mathbf{p}_{_T}^2 + M_{_C}^2}\, e^{-\alpha_{_T}\mathbf{p}_{_T}^2}\, f_1^f(x)\;, \tag{24}$$

where $\alpha_{_T} = 1$ GeV^{-2}. Then, the c_4 coefficient turns out to be (see Sec. VI of Ref. [34] for all details):

$$c_4(q_{_T}, x_{\bar{p}}, x_p) = -\frac{2q_{_T}M_{_C}}{4M_{_C}^2 + q_{_T}^2} \frac{\sum_f e_f^2 \, \bar{f}_1^f(x_{\bar{p}}) \, h_1^f(x_p)}{\sum_f e_f^2 \, \bar{f}_1^f(x_{\bar{p}}) \, f_1^f(x_p)} \, . \tag{25}$$

For sake of simplicity, we assume that we can approximate the contribution of each flavor to the parton distributions by a corresponding average function, such that we finally get

$$c_4(q_{_T}, x_{\bar{p}}, x_p) \sim -\frac{2q_{_T}M_{_C}}{4M_{_C}^2 + q_{_T}^2} \frac{\langle \bar{f}(x_{\bar{p}}) \rangle \, \langle h_1(x_p) \rangle}{\langle \bar{f}(x_{\bar{p}}) \rangle \, \langle f_1(x_p) \rangle} \equiv -\frac{2q_{_T}M_{_C}}{4M_{_C}^2 + q_{_T}^2} \frac{\langle h_1(x_p) \rangle}{\langle f_1(x_p) \rangle} \, . \tag{26}$$

In order to disentangle the various azimuthal parts in the cross section, the most straightforward way is to integrate the corresponding azimuthal asymmetry with a proper weight depending on ϕ. However, if the $\sin(3\phi - \phi_{S_2})$ contribution to Eq. (10) is assumed small, a simpler procedure is available. In fact, for the remaining leading-twist contributions

$$\begin{aligned} P_1(\phi) &= \cos 2\phi \, , \\ P_2(\phi) &= \sin(\phi - \phi_{S_p}) \, , \\ P_3(\phi) &= \sin(\phi + \phi_{S_p}) \, , \end{aligned} \tag{27}$$

it is possible to show that for each bin x_p the asymmetry between the subsets of positive and negative values of $P_i(\phi)$ (spanning the whole ϕ range) does not depend on P_j for $j \neq i$. In the following Section, results will be presented and commented for azimuthal asymmetries constructed in this way for $P_1(\phi)$ and $P_3(\phi)$. Two choices with opposite features will be selected for the ratio $\langle h_1(x_p) \rangle / \langle f_1(x_p) \rangle$, namely the ascending function $2x_p$ and the descending one $2(1 - x_p)$. The goal is to determine the minimum number of events (compatible with the kinematical setup and cutoffs) required to produce azimuthal asymmetries that can be clearly distinguished like the corresponding originating distributions. In fact, this would be equivalent to state that some analytic information on $h_1(x)$ could be extracted from such spin asymmetry measurements.

D. Polarized target and dilution factor

When the transversely polarized proton is considered as a fixed target, in reality we assume a NH_3 target with 85% transverse polarization for the H nucleus. In the ideal conditions of scattering from a black sphere, the N hadronic cross section is exactly ten times bigger than the one for H, i.e. 390 mb [53]. This means that, from the point of view of hadronic collisions, the N nucleus is equivalent to 5 protons and 5 neutrons with no difference between protons and neutrons. In reality, this picture can be valid only at very small $x_{\bar{p}}$ and x_p, where the valence quarks do not dominate. However, as it is clear from Fig. 3 this domain is not accessible to our simulation. Rather, the events are concentrated at $x_i > 0.1$, $i = \bar{p}, p$, where the valence distributions are dominant and the annihilation occurs between a quark and an antiquark of the same flavor. Hence, the antiproton of the beam "prefers" to hit protons rather than neutrons. A convenient estimate would be to assume that in the NH_3 target the N nucleus behaves like if it was made of 5 protons and 4 neutrons, such that out of 12 events, 9 come from collisions inside N and 3 inside H_3. Therefore, in the scatter plot of Fig. 3 with 48000 events, only 12000 are related to H_3 with 85% of transverse polarization, while 36000 are produced on the unpolarized N nucleus. The Monte-Carlo simulation takes into account such a combination of dilution factors.

When the $\bar{p}\, p^{\uparrow} \to \mu^+ \, \mu^- \, X$ process is considered as the collision of two beams, a systematic dilution factor 0.85 is applied to the proton polarization. The statistics of the simulation greatly benefits from this weaker dilution and, in fact, a much smaller sample of events is needed to get reasonable results, as it will become evident in the next Section.

IV. RESULTS

In this Section, we present results of a Monte-Carlo simulation for the $\bar{p}\, p^{\uparrow} \to \mu^+ \, \mu^- \, X$ and $\bar{p}\, p \to \mu^+ \, \mu^- \, X$ processes in order to make realistic estimates of the minimum number of events required to extract as detailed information as possible on the chiral-odd distributions h_1 and $h_1^{\perp}$. First, we consider an antiproton beam of 40 GeV energy hitting a fixed proton target and producing muon pairs with invariant mass in the range 4 GeV $\leq M \leq$ 9 GeV and total transverse momentum $q_{_T} > 1$ GeV/c. Then, we will select the lower antiproton beam energy of 15 GeV with the dilepton invariant mass in the range 1.5 GeV $\leq M \leq$ 2.5 GeV and we will explore both possibilities of a fixed proton

TABLE I: Total absorption cross sections per nucleon for antiprotons at the indicated energies and for various invariant masses of the Drell-Yan pair (see text for a discussion of the kinematics and the cutoffs).

$E_{\bar{p}}$ (GeV)	mode	event sample	M (GeV)	σ_{tot} (nb/nucleon)
40	fixed target	40000	$4 \div 9$	0.02
40	fixed target	40000	$1.5 \div 2.5$	1.6
15	fixed target	40000	4	4×10^{-4}
15	fixed target	40000	$1.5 \div 2.5$	0.8
15	collider	8000	$4 \div 9$	0.1
15	collider	8000	$1.5 \div 2.5$	2.4

target and of a collision with a proton beam of 3.3 GeV energy, such that the cm available squared energy is $s \sim 200$ GeV^2 (see Sec. III A). For fixed targets at such low energy, the QPM picture leading to Eq. (12), or (13), is not well justified because of the unavoidable corrections due to higher-twist contributions. But we stress that the primary goal of this simulation is to explore the feasibility of the extraction of the h_1 and $h_1^\perp$ distributions, not to make a precision calculation. Hence, we will retain the same approach in all kinematical cases above described.

The transversely polarized proton target is obtained from a NH_3 molecule where each H nucleus is 85% transversely polarized and the number of "polarized" collisions with each H nucleus is 25% of the total number of collisions. The events are sorted according to the cross section of Eq. (13) (reduced by the above dilution factor) and supplemented by Eqs. (17) and (19)-(26). In the following, we will study the azimuthal asymmetries generated by the $\cos 2\phi$ and $\sin(\phi + \phi_{S_p})$ dependences in the cross section (see Eqs. (5), (10), (20) and (22)). For each x_p bin, the asymmetry is constructed by dividing the sample in two groups, one for positive values in the ϕ dependence (U) and another one for negative values (D), and taking the ratio $(U - D)/(U + D)$; the azimuthal ϕ dependence is considered in the Collins-Soper frame.

We have initially taken samples of 100000 and 20000 events for fixed target and collider modes, respectively. The above cuts in M and $q_{_T}$ are implemented also by a restriction on the θ angular dependence to the range 60 deg. $< \theta <$ 120 deg., where events are mostly concentrated; outside these limits, in fact, the azimuthal asymmetries are too small. Analogously, as a general rule x_p bins with less than 100 events are considered empty. All these cuts reduce the starting samples approximately by a factor 2.5; conventionally, we will indicate the surviving 40000 and 8000 events, respectively, as "good" events. Statistical errors for the above mentioned azimuthal asymmetry $(U - D)/(U + D)$ are obtained by making 20 independent repetitions of the simulation for each considered case, and then calculating for each x_p bin the average asymmetry value and the variance. We checked that 20 repetitions are a reasonable threshold to have stable numbers, since the results do not change significantly when increasing the repetitions from 6 to 20.

From our Monte-Carlo results, we deduce a total cross section $\sigma_{tot} = 0.02$ nb per single nucleon for the absorption of antiprotons in a 40 GeV beam hitting a polarized NH_3 target in the above discussed conditions and producing final lepton pairs with invariant mass $M \geq 4$ GeV. This cross section is 2×10^9 times smaller than the total nucleon absorption cross section per single nucleon at the considered energy and under the conditions for a complete absorption, since the latter approximately amounts to 40 mb. In other words, when the flux of actually absorbed antiprotons is deduced from the experimental setup, the above cross section states that one out of 2×10^9 such antiprotons produces a "good" event for the selected kinematics. In Tab. I, we list the total cross sections for all the explored kinematics and for various ranges of invariant masses. If $\mathcal{L}$ is the luminosity in units (cm^{-2}s^{-1}), the product $\sigma_{tot}\mathcal{L}$ gives the number of "good" events per nucleon and per second. For example, we deduce that in the collider mode for $1.5 \leq M \leq 2.5$ GeV we would approximately get 60000 "good" events/month with $\mathcal{L} = 10^{31}$ (cm^{-2}s^{-1}).

A. Polarized Drell-Yan

In Fig. 5, the sample of 40000 "good" events for the $\bar{p}\, p^\uparrow \to \mu^+ \mu^- X$ process is displayed for the antiproton beam energy $E_{\bar{p}} = 40$ GeV and for the case of a fixed proton target. The left panel corresponds to the choice $\langle h_1(x_p)\rangle / \langle f_1(x_p)\rangle = 2x_p$, while the right one to the function $2(1 - x_p)$, according to Eq. (26). Results are reported in x_p bins over the entire range, but the bins at the boundaries, corresponding to $x_p < 0.2$ and $x_p > 0.8$, are scarcely or not at all populated, according to the phase space distribution of Fig. 3. For each bin, two groups of events are stored: one corresponding to positive values of $\sin(\phi + \phi_{S_p})$ in Eqs. (20) and (22) (represented by the darker histogram), the other one corresponding to negative values (represented by the superimposed lighter histogram).

In Fig. 6, the resulting asymmetry $(U - D)/(U + D)$, between cross sections with positive (U) and negative

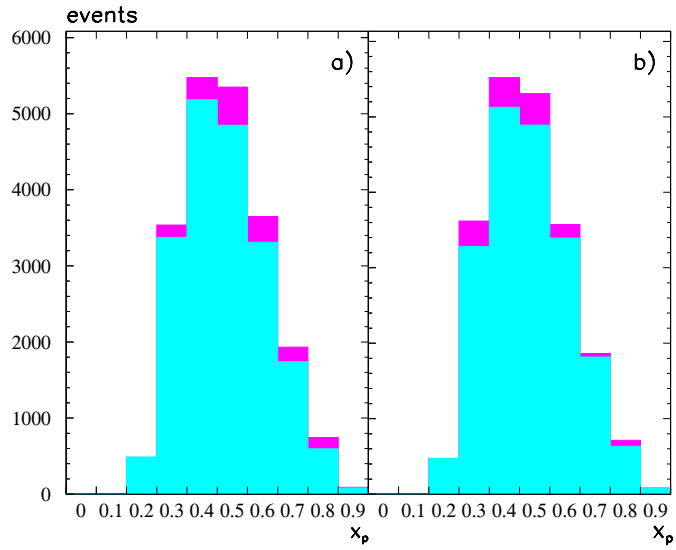

FIG. 5: The sample of 40000 events for the $\bar{p}\,p^{\uparrow} \to \mu^+\,\mu^-\,X$ process on a fixed proton target with an antiproton beam energy $E_{\bar{p}} = 40$ GeV and with a muon pair of invariant mass $4 \leq M \leq 9$ GeV and transverse momentum $q_T > 1$ GeV/c (for further details on the cutoffs, see text). a) Left panel for the choice $\langle h_1(x_p)\rangle/\langle f_1(x_p)\rangle = 2x_p$ (brackets mean that each flavor contribution in the numerator is replaced by a common average term, similarly in the denominator; for further details, see text). b) Right panel for $\langle h_1(x_p)\rangle/\langle f_1(x_p)\rangle = 2(1-x_p)$. For each bin, the darker histogram corresponds to positive values of $\sin(\phi + \phi_{S_p})$ in Eqs. (20) and (22), the superimposed lighter one to negative values.

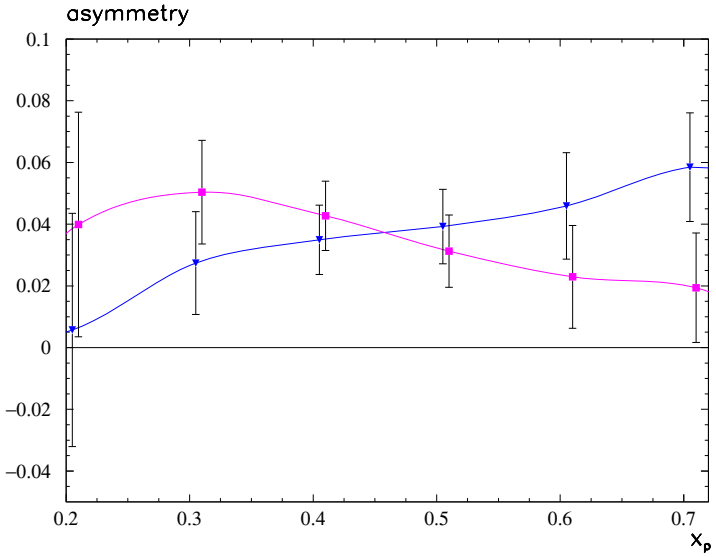

FIG. 6: Azimuthal asymmetry $(U - D)/(U + D)$ between cross sections in the previous figure corresponding to the darker histograms (U) and superimposed lighter histograms (D), as bins in x_p. Downward triangles for the case when $\langle h_1(x_p)\rangle/\langle f_1(x_p)\rangle = 2x_p$, squares when it equals $2(1 - x_p)$. Continuous lines are drawn to guide the eye. Error bars due to statistical errors only, obtained by 20 independent repetitions of the simulation (see text for further details).

(D) values of $\sin(\phi + \phi_{S_p})$, is plotted again in x_p bins for both choices: downward triangles for the case when $\langle h_1(x_p)\rangle/\langle f_1(x_p)\rangle = 2x_p$, squares when it equals $2(1 - x_p)$. The error bars represent statistical errors only.

Here and in the following cases, both functional forms for $\langle h_1(x_p)\rangle/\langle f_1(x_p)\rangle$, once integrated in x_p over the entire range, give the same overall size 1. Extrapolating information from other sources (lattice calculations, other experiments like semi-inclusive DIS, theoretical properties like the Soffer bound, etc..) suggests that this size may be a reasonable expectation [34]. From Fig. 6, we first conclude that 40000 "good" events of antiprotons with energy 40 GeV hitting fixed protons and producing muon pairs with $4 \leq M \leq 9$ GeV, are enough to produce a statistically

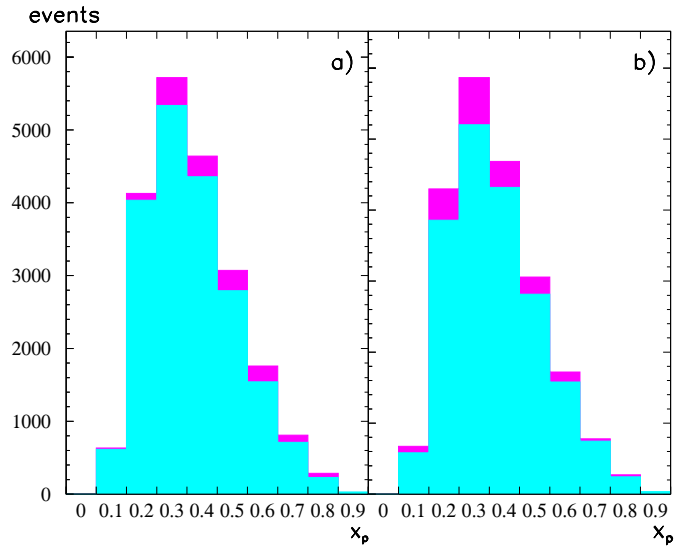

FIG. 7: Same as in Fig. 5 but with the antiproton beam energy $E_{\bar{p}} = 15$ GeV and with a muon pair of invariant mass $1.5 \leq M \leq 2.5$ GeV.

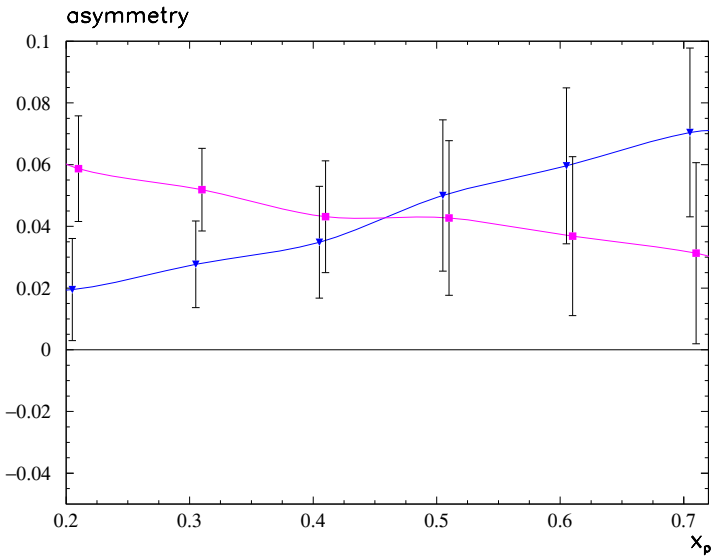

FIG. 8: Azimuthal asymmetry collected in x_p bins in the same kinematics as in Fig. 7 and with the same notations as in Fig. 6. Continuous lines are drawn to guide the eye. Error bars from statistical errors only.

nonvanishing azimuthal asymmetry of about 5% on the average. But it is difficult to disentangle the two different functional forms of the ratio except for very high $x_p \gtrsim 0.6$, where the QPM picture becomes questionable. Equivalently, it is difficult to extract unambiguous information on the transversity distribution $h_1(x)$. Moreover, from Tab. I we deduce that a luminosity $\mathcal{L} = 10^{31}$ cm^{-2}s^{-1} would give a rate of 500 "good" events/month. The same conclusion holds if the absolute size of the ratio is expected in the range $0.5 \div 1$. Only a smaller number by an order of magnitude would imply a much larger sample of events in order to reach the same sensitivity.

The situation is somewhat better at the lower antiproton beam energy $E_{\bar{p}} = 15$ GeV, because in the scatter plot (analogous of Fig. 3) the lowest cutoff in $\tau = x_p x_{\bar{p}} = M^2/s$ is smaller since now $1.5 \leq M \leq 2.5$ GeV. The highest density of events (and the best statistics) is now reached at lower values of x_p. In fact, while in Fig. 7 we show the usual sample of 40000 "good" events in the same conditions and notations as in Fig. 5 but for $E_{\bar{p}} = 15$ GeV and $1.5 \leq M \leq 2.5$ GeV, in Fig. 8 the resulting azimuthal asymmetry (again, with the same notations as in Fig. 6) clearly shows how the ascending (descending) behaviour of $\langle h_1(x_p)\rangle/\langle f_1(x_p)\rangle = 2x_p\,[2(1-x_p)]$ reflects in the corresponding

asymmetry making the two results statistically distinguishable for $x_p \lesssim 0.4$ (and, approximately, also for very high values $x_p \gtrsim 0.7$).

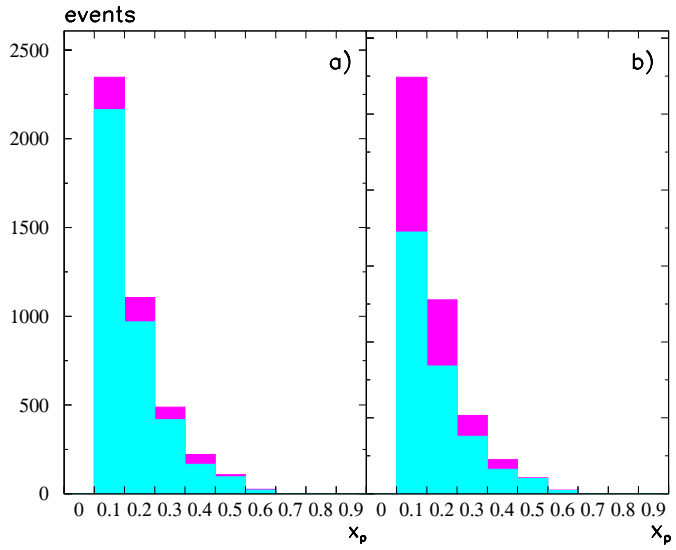

FIG. 9: The sample of 8000 events for the $\bar{p}\,p^{\uparrow} \to \mu^+\,\mu^-\,X$ process where an antiproton beam with energy $E_{\bar{p}} = 15$ GeV collides on a proton beam with energy $E_p = 3.3$ GeV producing muon pairs with invariant mass $4 \leq M \leq 9$ GeV and transverse momentum $q_T > 1$ GeV/c (for further details on the cutoffs, see text). The content of each panel and the notations are as in Fig. 5.

The lowest range in the muon pair invariant mass offers also a faster rate in the collection of "good" events. From Tab. I, we deduce that with the above mentioned luminosity $\mathcal{L} = 10^{31}$ cm^{-2}s^{-1} it should be possible to collect a sample 40 times bigger than in the previous case, namely 20000 "good" events/month; or, equivalently, to reach the same counts (500 "good" events/month) with $\mathcal{L} = 2.5 \times 10^{29}$ cm^{-2}s^{-1}.

From previous examples, it seems evident that the smaller the lower cutoff in τ, the lower the range in x_p where the highest density of events gives the best available statistics to extract as many details as possible about h_1. Since $\tau = M^2/s$ and we want no overlap with M values corresponding to hadronic resonances whose elementary mechanism for the production of the final muon pair is not well under control, it might be convenient to considerably increase s. The most effective way is to consider the proton not as a fixed target but as a beam colliding against the antiproton one. Keeping for the latter the energy $E_{\bar{p}} = 15$ GeV, a proton beam with $E_p = 3.3$ GeV produces an available cm squared energy $s = 200$ GeV^2 (see Sec. III A for details). In Fig. 9, a sample of 8000 "good" events for the $\bar{p}\,p^{\uparrow} \to \mu^+\,\mu^-\,X$ process leading to muon pairs with invariant mass $4 \leq M \leq 9$ GeV is plotted in x_p bins, all the notations and the other cutoffs being the same as before. Evidently, events are concentrated at lower x_p bins; but also the asymmetry is, as it can be deduced from the different color codes of the histograms. In fact, in Fig. 10 the corresponding azimuthal asymmetry $(U - D)/(U + D)$ is plotted again with the same notations as in Fig. 6, the x_p bins being limited to 0.6 because the histograms corresponding to higher x_p values are empty. First of all, the absolute size of such asymmetry is much bigger (note the different scale with respect to Figs. 6 and 8); on the average, it is approximately 15%. But, most important, the best statistics is achieved for $x_p \lesssim 0.4$, where the small error bars allow for a very clean distinction between the results corresponding to the opposite trends for the function $\langle h_1(x_p)\rangle/\langle f_1(x_p)\rangle$. And all this can be obtained with a reduced sample of just 8000 "good" events.

In conclusion, although the option of a fixed proton target permits a sufficiently clean extraction of the analytic properties of the function $h_1(x)$ for $x \lesssim 0.4$ provided that the invariant mass of the final muon pair is enough low, the collider mode seems more promising. The higher available cm energy grants a cleaner theoretical description of the elementary mechanism, gives bigger azimuthal asymmetries, and allows for a much better statistics and a clean information in the same range $x \lesssim 0.4$. As for the event rate, from Tab. I we deduce that the luminosity $\mathcal{L} = 10^{31}$ cm^{-2} s^{-1} would allow to collect 2500 "good" events/month.

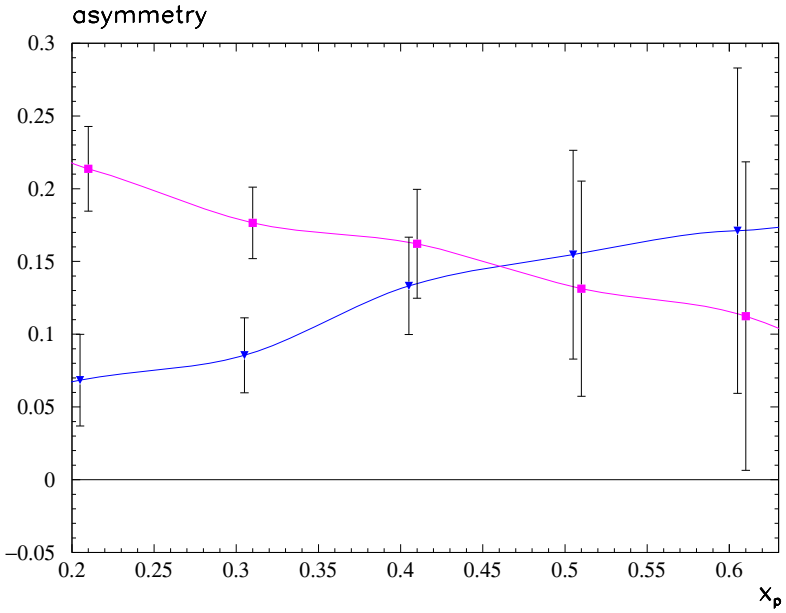

FIG. 10: Azimuthal asymmetry collected in x_p bins in the same kinematics as in Fig. 9 and with the same notations as in Fig. 6. Continuous lines are drawn to guide the eye. Error bars from statistical errors only.

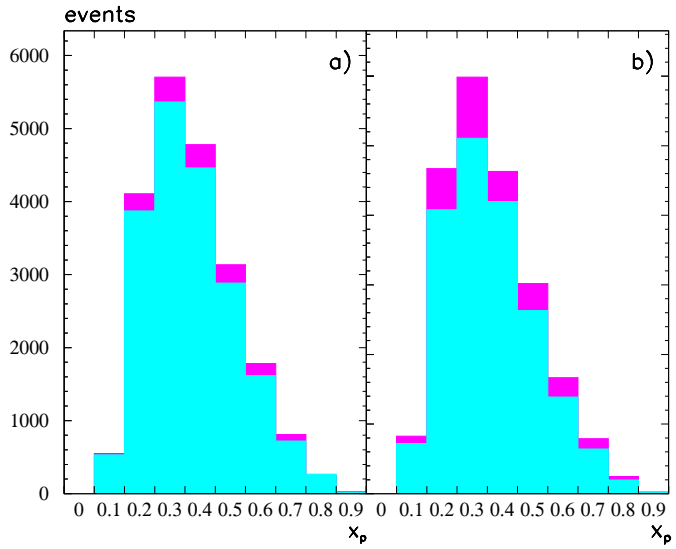

FIG. 11: The sample of 40000 events for the unpolarized $\bar{p}\,p \to \mu^+\,\mu^-\,X$ process on a fixed NH_3 target with an antiproton beam energy $E_{\bar{p}} = 15$ GeV and with a muon pair of invariant mass $1.5 \leq M \leq 2.5$ GeV (for further details on the cutoffs, see text). a) Left panel for $1 < p_T < 2$ GeV/c. b) Right panel for $2 < p_T < 3$ GeV/c. For each bin, the darker histogram corresponds to positive values of $\cos 2\phi$ in Eq. (20), the superimposed lighter one to negative values.

B. Unpolarized Drell-Yan

In Fig. 11, the sample of 40000 "good" events for the unpolarized $\bar{p}\,p \to \mu^+\,\mu^-\,X$ process is displayed for the case of a fixed NH_3 target and for the antiproton beam energy $E_{\bar{p}} = 15$ GeV, i.e. in the same initial conditions proposed at the HESR at GSI by the PANDA collaboration [54]. The muon pair invariant mass is constrained by $1.5 \leq M \leq 2.5$ GeV and 60 deg. $< \theta <$ 120 deg. The left panel corresponds to muon pairs with transverse momentum $1 < p_T < 2$ GeV/c, while the right one to the choice $2 < p_T < 3$ GeV/c. The goal is to test the simple q_T distribution assumed for the coefficient ν in Eq. (21) which leads to the corresponding factorized contribution in Eq. (20). For each bin,

two groups of events are stored corresponding to positive (darker histograms, U) and negative (superimposed lighter histograms, D) values of $\cos 2\phi$ in Eq. (20). Again, as in previous plots results are reported in x_p bins over the entire range, but the bins at the boundaries, corresponding to $x_p < 0.2$ and $x_p > 0.8$, are scarcely or not at all populated and they will be discarded in the plot of the corresponding azimuthal asymmetry $(U - D)/(U + D)$.

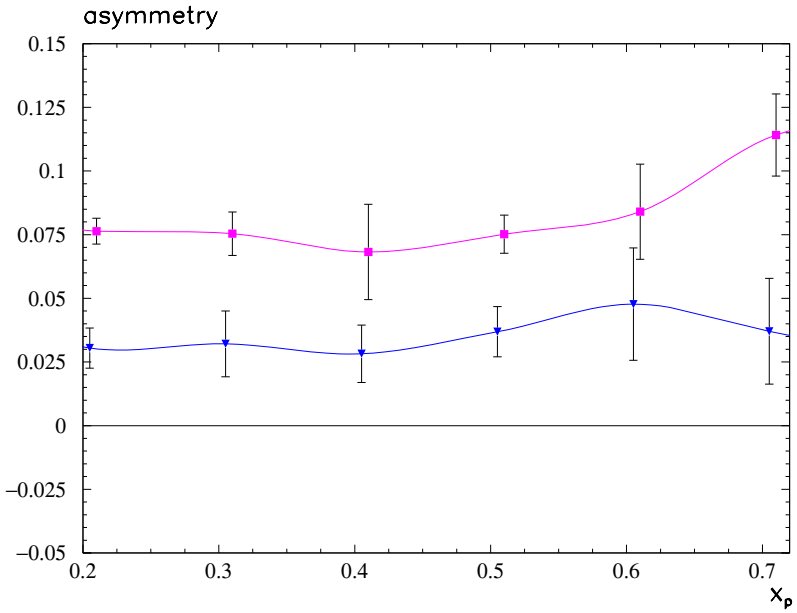

FIG. 12: Azimuthal asymmetry $(U - D)/(U + D)$ between cross sections in the previous figure corresponding to the darker histograms (U) and superimposed lighter histograms (D), as bins in x_p. Downward triangles for muon pairs with transverse momentum $1 < p_T < 2$ GeV/c, squares for $2 < p_T < 3$ GeV/c. Continuous lines are drawn to guide the eye. Error bars due to statistical errors only.

In Fig. 12, the resulting asymmetry $(U - D)/(U + D)$ between cross sections with positive (U) and negative (D) values of $\cos 2\phi$ in Eq. (20), is sorted in x_p. This asymmetry, already observed at higher energy [40], is responsible for the violation of the so-called Lam-Tung sum rule and, according to Eq. (5), it could be related to the distribution function $h_1^\perp$, namely it could be interpreted as a distortion of the parton momentum distribution due to its transverse polarization. The predictions of Fig. 12 should be reliable, because the function $\nu(q_T)$ has been tested against the most recent available measurements [40]. In fact, despite its simple functional dependence $\nu(q_T)$ should not depend on the energy; therefore, even with an antiproton beam of 15 GeV the expected size of the asymmetry should be the one displayed in Fig. 12. Moreover, in the unpolarized Drell-Yan the magnitude of the asymmetry should also not depend on the target, because there is no dilution factor as it is the case for the corresponding polarized process. Nevertheless, in Fig. 12 two different sets of asymmetries are plotted corresponding to different ranges for the transverse momentum of the final muon pair: downward triangles for $1 < p_T < 2$ GeV/c and squares for $2 < p_T < 3$ GeV/c. The good statistics and the small error bars should allow to reliably test the q_T dependence assumed for the coefficient ν in Eq. (21).

V. CONCLUSIONS

In this paper, we have concentrated on the investigation of the spin structure of the proton using the single-polarized Drell-Yan process $\bar{p}p^\uparrow \to l^+l^-X$. At leading twist, the polarized part of the cross section contains three contributions with different dependences on the azimuthal angle ϕ identifying the direction of the final muon pair [34]. We have focussed on the one involving the convolution of the transversity distribution, the missing piece necessary to complete the knowledge of the nucleon spin structure at leading twist [6, 7], and the distribution $h_1^\perp$, which describes how in an unpolarized hadron the momentum distribution of a parton is distorted by its transverse polarization. Extraction of the latter is of great importance as well, because $h_1^\perp$ contains information on the orbital angular momentum of partons and it appears also at leading twist in the unpolarized part of the cross section, weighted by $\cos 2\phi$. As such, it is believed to be responsible for the well known violation of the Lam-Tung sum rule [38, 39, 40], an anomalous big azimuthal asymmetry of the unpolarized Drell-Yan cross section, that neither NLO QCD calculations [41], nor higher

twists or factorization-breaking terms in NLO QCD [42, 43, 44] are able to justify. Measuring at the same time the azimuthal asymmetries of the unpolarized and single-polarized Drell-Yan cross section allows to determine both the unknown functions, i.e. the transversity and $h_1^\perp$.

Using unpolarized antiproton beams offers the advantage of involving (anti)parton valence distributions that should not be suppressed as in the standard fully polarized Drell-Yan [27, 28], but avoiding at the same time the difficulty of polarizing antiprotons. At GSI a new facility is under development, the High Energy Storage Ring (HESR), where an antiproton source will be built. The transversely polarized proton target could be obtained from a NH_3 molecule where each H nucleus, for example, is 85% transversely polarized; a further 25% dilution factor needs to be applied to filter out spurious unpolarized events from the N nucleus. We have simulated the above single-polarized Drell-Yan process using an antiproton beam of 40 GeV and selecting muon pairs with invariant mass M in the range $4 \div 9$ GeV and with a total transverse momentum above 1 GeV/c. In this kinematics, the quark-antiquark pair annihilates into a virtual photon and the theoretical description of the elementary process is well under control. We have also made simulations at the lower beam energy of 15 GeV but with invariant masses in the range $1.5 \div 2.5$ GeV, in order to keep a reasonably large phase space and at the same time to avoid the overlap with hadronic resonances like the ϕ at 1 GeV and the J/ψ at 3.1 GeV. For such low M values, the parton model interpretation of the elementary annihilation is questionable because of the contributions of higher twists. But from the analysis of the scatter plot events seem to concentrate at the lowest possible values of $\tau = x_p x_{\bar{p}} = M^2/s$ (where $x_p, x_{\bar{p}}$, are the fractions of hadron momenta carried by the annihilating quark-antiquark pair and s is the available initial squared energy in the center-of-mass system); hence, the simulation is still useful to study the gross features of the cross section and to explore the possibility of extracting the transversity distribution at this lower energy. For both beam energies, the polar-angle distribution of the muon pairs is restricted to the range $60 \div 120$ deg., where most of the Monte-Carlo events are concentrated. An alternative way to reach the high-statistics portion of the phase space at low τ is to increase s. Therefore, we have considered also the option where the antiproton beam with energy $E_{\bar{p}} = 15$ GeV collides on a proton beam with $E_p = 3.3$ GeV such that $s = 200$ GeV^2. In this last case, $4 \leq M \leq 9$ GeV, all the other applicable cutoffs being unchanged.

The primary goal of the simulation is to estimate the number of events required in order to access unambiguous information on the distribution functions of interest. Azimuthal asymmetries have been built, for each bin in the partonic momentum fraction, by separating the cross sections with positive values in the ϕ dependence from the negative ones and taking the ratio between the difference and the sum of such values. The $\cos 2\phi$ asymmetry in the unpolarized cross section has already been measured [40] at higher energies. However, under the present kinematical conditions the magnitude of the asymmetry should be independent from the energy of the experiment and it can be used as a cross-check of the Monte-Carlo simulation. It turns out that with an initial sample of 40000 events (surviving the filter of the various discussed cutoffs) it is possible to study in detail the function ν responsible for such an asymmetry, but in the restricted range $0.2 \div 0.8$ for the parton momentum fraction, because the boundary bins are not enough populated.

In the case where antiprotons with energy 40 GeV hit transversely polarized fixed proton targets and produce muon pairs with $4 \leq M \leq 9$ GeV, the 40000 events are enough to produce a statistically nonvanishing azimuthal asymmetry of about 5% on the average, but it seems difficult to extract more detailed information on the analytic structure of $h_1(x)$ except for very high $x \gtrsim 0.6$, where the adopted QPM picture becomes questionable. The lower invariant mass range $1.5 \leq M \leq 2.5$ GeV allows to reach lower values of τ in the phase space, where most of the events are concentrated, even for lower antiproton beam energies such as 15 GeV. Hence, a better statistics is reached for lower x_p values and it seems possible both to extract the functional dependence of $h_1(x)$ for $x \lesssim 0.4$, and to collect events at a higher rate (several times bigger than the previous case at the same luminosity). However, the best option seems the one where antiproton and proton beams collide reaching high values of s. In the explored case $s = 200$ GeV^2, the theoretical description of the elementary mechanism is clean and is not affected by complications like, e.g., higher twists; moreover, the absolute size of the azimuthal asymmetry turns out bigger and the much better statistics should allow for an unambiguous extraction of $h_1(x)$ for $x \lesssim 0.4$ with a reduced sample of just 8000 events.

In conclusion, we hope that the present work will help in the feasibility studies about the physics program of hadronic collisions with antiproton beams at the HESR at GSI.

---

[1] G. Bunce et al., Phys. Rev. Lett. **36**, 1113 (1976).
[2] D. L. Adams et al. (FNAL-E704), Phys. Lett. **B264**, 462 (1991).
[3] J. Adams et al. (STAR), Phys. Rev. Lett. **92**, 171801 (2004), hep-ex/0310058.
[4] G. L. Kane, J. Pumplin, and W. Repko, Phys. Rev. Lett. **41**, 1689 (1978).
[5] J. P. Ralston and D. E. Soper, Nucl. Phys. **B152**, 109 (1979).
[6] X. Artru and M. Mekhfi, Z. Phys. **C45**, 669 (1990).

[7] R. L. Jaffe and X. Ji, Phys. Rev. Lett. **67**, 552 (1991).
[8] R. L. Jaffe (1996), proceedings of the Ettore Majorana International School on the Spin Structure of the Nucleon, Erice, Italy, 3-10 Aug 1995., hep-ph/9602236.
[9] V. Barone and P. G. Ratcliffe, *Transverse Spin Physics* (World Scientific, River Edge, USA, 2003).
[10] R. L. Jaffe and X. Ji, Phys. Rev. Lett. **71**, 2547 (1993), hep-ph/9307329.
[11] A. Bravar (Spin Muon), Nucl. Phys. **A666**, 314 (2000).
[12] A. Airapetian et al. (HERMES), Phys. Rev. Lett. **84**, 4047 (2000), hep-ex/9910062.
[13] A. Airapetian et al. (HERMES), Phys. Rev. **D64**, 097101 (2001), hep-ex/0104005.
[14] A. Airapetian et al. (HERMES), Phys. Lett. **B562**, 182 (2003), hep-ex/0212039.
[15] A. Airapetian et al. (HERMES) (2004), hep-ex/0408013.
[16] U. Elschenbroich, G. Schnell, and R. Seidl (HERMES) (2004), hep-ex/0405017.
[17] P. J. Mulders and R. D. Tangerman, Nucl. Phys. **B461**, 197 (1996), erratum-ibid. **B484** (1996) 538, hep-ph/9510301.
[18] D. Boer, P. J. Mulders, and F. Pijlman, Nucl. Phys. **B667**, 201 (2003), hep-ph/0303034.
[19] J. C. Collins, Phys. Lett. **B536**, 43 (2002), hep-ph/0204004.
[20] A. Metz, Phys. Lett. **B549**, 139 (2002), hep-ph/0209054.
[21] C. J. Bomhof, P. J. Mulders, and F. Pijlman, Phys. Lett. **B596**, 277 (2004), hep-ph/0406099.
[22] J. Collins and A. Metz (2004), hep-ph/0408249.
[23] F. Yuan, Phys. Lett. **B589**, 28 (2004), hep-ph/0310279.
[24] L. P. Gamberg, D. S. Hwang, and K. A. Oganessyan, Phys. Lett. **B584**, 276 (2004), hep-ph/0311221.
[25] A. Bacchetta, P. J. Mulders, and F. Pijlman (2004), hep-ph/0405154.
[26] H. Avakian (CLAS) (2003), hep-ex/0301005.
[27] O. Martin, A. Schafer, M. Stratmann, and W. Vogelsang, Phys. Rev. **D57**, 3084 (1998), hep-ph/9710300.
[28] V. Barone, T. Calarco, and A. Drago, Phys. Rev. **D56**, 527 (1997), hep-ph/9702239.
[29] PAX Collab., Letter of Intent for *Antiproton-Proton Scattering Experiments with Polarization*, Spokespersons: F. Rathmannn and P. Lenisa (2004), http://www.fz-juelich.de/ikp/pax/.
[30] ASSIA Collab., Letter of Intent for *A Study of Spin-dependent Interactions with Antiprotons: the Structure of the Proton*, Spokesperson: R. Bertini (2004), http://www.gsi.de/documents/DOC-2004-Jan-152-1.ps.
[31] A. V. Efremov, K. Goeke, and P. Schweitzer, Eur. Phys. J. **C35**, 207 (2004), hep-ph/0403124.
[32] M. Anselmino, V. Barone, A. Drago, and N. N. Nikolaev, Phys. Lett. **B594**, 97 (2004), hep-ph/0403114.
[33] M. Radici (2004), hep-ph/0407085.
[34] D. Boer, Phys. Rev. **D60**, 014012 (1999), hep-ph/9902255.
[35] D. W. Sivers, Phys. Rev. **D43**, 261 (1991).
[36] A. V. Efremov, K. Goeke, and P. Schweitzer, Phys. Lett. **B568**, 63 (2003), hep-ph/0303062.
[37] M. Anselmino et al. (2004), hep-ph/0408356.
[38] S. Falciano et al. (NA10), Z. Phys. **C31**, 513 (1986).
[39] M. Guanziroli et al. (NA10), Z. Phys. **C37**, 545 (1988).
[40] J. S. Conway et al., Phys. Rev. **D39**, 92 (1989).
[41] A. Brandenburg, O. Nachtmann, and E. Mirkes, Z. Phys. **C60**, 697 (1993).
[42] A. Brandenburg, S. J. Brodsky, V. V. Khoze, and D. Muller, Phys. Rev. Lett. **73**, 939 (1994), hep-ph/9403361.
[43] K. J. Eskola, P. Hoyer, M. Vanttinen, and R. Vogt, Phys. Lett. **B333**, 526 (1994), hep-ph/9404322.
[44] E. L. Berger and S. J. Brodsky, Phys. Rev. Lett. **42**, 940 (1979).
[45] J. C. Collins and D. E. Soper, Phys. Rev. **D16**, 2219 (1977).
[46] D. Boer and P. J. Mulders, Phys. Rev. **D57**, 5780 (1998), hep-ph/9711485.
[47] G. Moreno et al., Phys. Rev. **D43**, 2815 (1991).
[48] J. C. Collins, Nucl. Phys. **B396**, 161 (1993), hep-ph/9208213.
[49] E. Anassontzis et al., Phys. Rev. **D38**, 1377 (1988).
[50] G. Altarelli, R. K. Ellis, and G. Martinelli, Nucl. Phys. **B157**, 461 (1979).
[51] E. L. Berger (1982), invited review given at Fermilab Workshop on Drell-Yan Processes, Batavia, Ill., Oct 7-8, 1982.
[52] A. J. Buras and K. J. F. Gaemers, Nucl. Phys. **B132**, 249 (1978).
[53] E. Segre, *Nuclei and Particles* (W.A. Benjamin Inc., New York, 1977).
[54] PANDA Collab., Letter of Intent for the *Proton-Antiproton Darmstadt Experiment*, Spokesperson: U. Wiedner (2004), http://www.gsi.de/documents/DOC-2004-Jan-115-1.pdf.